ELSEVIER

Journal of Hazardous Materials A139 (2007) 1–8

Journal of Hazardous Materials

www.elsevier.com/locate/jhazmat

The rate of pressure rise of gaseous propylene–air explosions in spherical and cylindrical enclosures

Domnina Razus [a,*], Codina Movileanua [a], Dumitru Oancea [b]

[a] *"Ilie Murgulescu" Institute of Physical Chemistry, 202 Spl. Independentei, P.O. Box 12-194, 060021 Bucharest, Romania*
[b] *Department of Physical Chemistry, University of Bucharest, 4-12 Regina Elisabeta Blvd., 030018 Bucharest, Romania*

Received 3 March 2006; received in revised form 23 May 2006; accepted 31 May 2006
Available online 6 June 2006

Abstract

The maximum rates of pressure rise of propylene–air explosions at various initial pressures and various fuel/oxygen ratios in three closed vessels (a spherical vessel with central ignition and two cylindrical vessels with central or with top ignition) are reported. It was found that in explosions of quiescent mixtures the maximum rates of pressure rise are linear functions on total initial pressure, at constant initial temperature and fuel/oxygen ratio. The slope and intercept of found correlations are greatly influenced by vessel's volume and shape and by the position of the ignition source — factors which determine the amount of heat losses from the burned gas in a closed vessel explosion. Similar data on propylene–air inert mixtures are discussed in comparison with those referring to propylene–air, revealing the influence of nature and amount of inert additive. The deflagration index K_G of centrally ignited explosions was also calculated from maximum rates of pressure rise.

Keywords: Explosion; Closed vessel; Rate of pressure rise; Deflagration index; Propylene combustion; Inert additive

1. Introduction

The maximum rate of pressure rise during a closed vessel explosion, $(dp/dt)_{max}$, is defined as the highest value of pressure rise rate observed at a given fuel concentration, under specific initial temperature and pressure conditions [1]. Besides the explosion pressure, the maximum rate of pressure rise is one of the most important safety parameters for assessing the hazard of a process and for design of vessels able to withstand an explosion or of vents used as relief devices of enclosures against damages produced by gaseous explosions [2–5].

Maximum rates of pressure rise are used for calculating the severity factor (or "deflagration index") K_G, of gas explosions in enclosures:

$$K_G = \sqrt[3]{V}\left(\frac{dp}{dt}\right)_{max} \quad (1)$$

defined by analogy to the severity factor of dust–air explosions, K_{st}, introduced by Bartknecht and Zwahlen [2]. For practical purposes, it was assumed that K_G is constant regardless of spherical vessel's volume V, depending only on the composition of fuel–oxidant mixture [2,3] so that K_G of gas mixtures at standard temperature and pressure may be used for scaling explosions in such vessels. Experimental evidence has shown that K_G increases much more as Eq. (1) accounts for, when V increases [3], but it is still a flammability index of wide interest.

Maximum rates of pressure rise in closed vessel explosions are influenced by the composition, pressure and temperature of the fuel–air mixture (factors which determine the rate of heat release) and by the volume and shape of the enclosure, the ignition source size, energy and position, the pre-existing or combustion-created turbulence (factors which determine the amount of generated heat as well as the amount of heat losses during flame propagation) [6–10].

The explosion pressure and the flame temperature of constant volume combustion can be determined by computation, based only on initial flammable mixture composition, pressure and temperature, assuming the flame propagation is adiabatic. In contrast, the maximum rate of pressure rise is not ready to be calculated without knowledge of heat release and heat transfer

* Corresponding author. Tel.: +40 21 316 79 12; fax: +40 21 312 11 47.
E-mail addresses: drazus@icf.ro, drazus@chimfiz.icf.ro (D. Razus), doan@gw-chimie.math.unibuc.ro (D. Oancea).

0304-3894/$ – see front matter © 2006 Elsevier B.V. All rights reserved.
doi:10.1016/j.jhazmat.2006.05.103

Nomenclature

h	height
K	deflagration index
p	pressure
S	burning velocity
t	time
T	temperature
V	volume

Subscripts

f	referring to flame
G	referring to gas
max	maximum value
s	referring to spherical vessel S
u	unburned gas
v	referring to spherical vessel V
0	referring to the initial state of mixture

Greek symbols

γ	adiabatic coefficient
μ	thermic exponent of burning velocity
ν	baric exponent of burning velocity
φ	equivalence ratio
Φ	diameter

rates from flame in various moments of its propagation. Earlier attempts of modelling the flame propagation inside a closed constant volume vessel were successful in predicting the peak pressure of explosion, but failed to predict the time to peak pressure and the rate of pressure rise in various stages of the process [11–14]. Later on, the development of comprehensive computer packages afforded accurate predictions of pressure evolution during explosions in enclosures in all stages, including those where the flame is close to the walls [15,16]. Some other studies were focused on modelling the flame propagation during the closed constant volume vessel, in order to compute the laminar burning velocity from the rate of pressure rise [16–18]. In a recent publication [19], adiabatic values of deflagration index $(K_G)_{max}$ were calculated for several reference fuel–air mixtures using a one-parameter correlation, based on the linear relationship derived by Lewis and von Elbe between the fraction of mass burned and pressure [20]. Such "upper limit values" are quite useful for practical purpose.

Many articles report experimental values of maximum rates of pressure rise and/or explosion index from measurements on homogeneous gaseous mixtures in spherical and in cylindrical enclosures [4,6–11,21–26]. Published data refer mainly to H_2–air [9,10], CH_4–air [2,4,9,10,16,23,25,26] and C_3H_8–air mixtures [9–11], but also to ethylene–air [9] and fluorinated derivatives of methane–air and ethylene–air [24,25] mixtures. Data were obtained in spherical vessels with various volumes, e.g. $V = 4.2$ L [25]; 5 L [2]; 20 L [4,10,16]; 40 L [26]; 120 L [10] and even 25 m^3 [6,7], in cylindrical vessels with low L/D ratio [10,11,26] or in elongated cylinders [8,9,23].

Such information is completed by the data in the present article: values of maximum rate of pressure rise and explosion index of propylene–air mixtures at various initial pressures and various fuel/oxygen ratios in three closed vessels: a spherical vessel with central ignition and two cylindrical vessels with central or top ignition. For several propylene–air mixtures, the adiabatic explosion index was calculated and compared to values derived from measurements in the spherical and cylindrical vessels with central ignition. Results on explosions of propylene–air mixtures in the presence of various amounts of argon, carbon dioxide and exhaust gas of propylene in air (burned gas from previous explosions) are also given and discussed, in connection to the nature and amount of additive.

2. Experimental

The experimental set-up contains a vacuum and gas-feed line, which interconnects the vacuum pump, the gas cylinders with fuel and air, the metallic cylinder for mixture storage and the explosion vessels. The vacuum pump maintains a vacuum of 0.1 mbar in the explosion vessel, after each experiment. The gas-feed line is tight at pressures between 0.1 mbar and 1.50 bar. More details were recently given [27,28].

Fuel–air, fuel–air inert and fuel–oxygen inert mixtures were obtained by the partial pressure method in gas cylinders and were used 24 h after mixing the components, at a total pressure of 4 bar. Propylene–air mixtures diluted with their own exhaust gas were prepared directly in the explosion vessel, according to the following steps: (a) the propylene–air mixture was admitted at a desired pressure then ignited and allowed to become quiescent; (b) the burned gas was evacuated down to the required partial pressure; (c) fresh propylene–air mixtures was added into the vessel and the new mixture (fuel–air + exhaust gas) was allowed 20 min to become homogeneous. After igniting and capturing the signals of the acquisition system, the burned gas was completely evacuated. A new cycle consists of burning the fuel–air mixture, evacuating the burned gas at a different partial pressure and preparing a new (fuel–air) + exhaust gas by adding fuel–air.

Experiments were performed in three explosion vessels, tight at vacuum and at pressures up to 40 bar: vessel S — a spherical vessel with the radius $R = 5$ cm; vessel C – a cylinder with $h = 15$ cm and $\Phi = 10$ cm and vessel V – a cylinder with $h = \Phi = 6$ cm. In vessel V only a limited number of experiments was made, using a stoichiometric propylene–air mixture. The initial pressure of explosive mixtures was measured using a strain gauge manometer Edwards EPSA-10HM.

Ignition was made with inductive–capacitive sparks produced between stainless steel electrodes by a standard auto induction coil; the spark gap was usually located in the geometrical centre of the vessel. Vessel C was fitted with a supplementary pair of electrodes, able to produce sparks 5 mm below the centre of the top lid. Both vessels S and C were equipped with an ionization probe used to monitor the arrival time of the flame front, mounted in equatorial position. The tip of an ionization probe was usually mounted 5 mm away from the wall. The sparks triggered the time-base of the acquisition system, by means of a low voltage signal.

The dynamic pressure was recorded with a piezoelectric transducer (Kistler 601A), connected to a Charge Amplifier (Kistler 5001SN). The signals of the ionization probe amplifier and of the Charge Amplifier were recorded with an acquisition data system TestLab^{TM} Tektronix 2505, by means of an acquisition card type AA1, at a rate of 5000 signals/s. The charge amplifier was calibrated by means of a Kistler Calibrator 5357.

Propylene (99.5%) was purchased from Arpechim Petrochemical Plant-Pitesti.

Oxygen (99.0%), Ar and CO_2 (99.5%) (SIAD, Italy) were used without further purification.

Air was dried by means of a line containing H_2SO_4, KOH (s), $CaCl_2$ and silica gel with moisture indicator.

Systems measured in the spherical bomb were: C_3H_6–air with an equivalence ratio $0.7 \leq \varphi \leq 1.3$; C_3H_6–O_2, stoichiometric, diluted with inert additives (CO_2, Ar); C_3H_6–air, stoichiometric with inert or inhibitor additives (CO_2, Ar, burned gases from previous explosions). Systems measured in cylindrical bomb C were: C_3H_6–air with $0.7 \leq \varphi \leq 1.3$. The system measured in cylindrical bomb V was C_3H_6–air with $\varphi = 1.0$.

The experimental procedure consisted of evacuating the combustion vessel down to 0.1 mbar; the fuel–air mixture was then introduced, allowed to become quiescent and ignited. Minimum three experiments were performed for each initial condition of explosive mixture. For a few systems (e.g. stoichiometric propylene–air), several sets of 15 experiments were conducted in identical conditions, in the spherical vessel with central ignition. The average error in measured explosion pressure was 2%.

A typical $p(t)$ diagram recorded during the explosion of a lean propylene–air mixture in spherical vessel S is shown in Fig. 1 together with the computed time derivative. The computation of (dp/dt) was made after smoothing the $p(t)$ data by Savitzky–Golay method, based on least squares quartic polynomial fitting across a moving window within the data. The method has the advantage of producing a smoothed first derivative without filtering the data. This involved the analysis of 500–700 points within $0 \leq t \leq \theta_{max}$. In all cases, we used a 10% smoothing level, since a higher value of this level (e.g. 20%) leads to a reduction of both noise and signal. The standard deviation of maximum rates of pressure rise calculated for

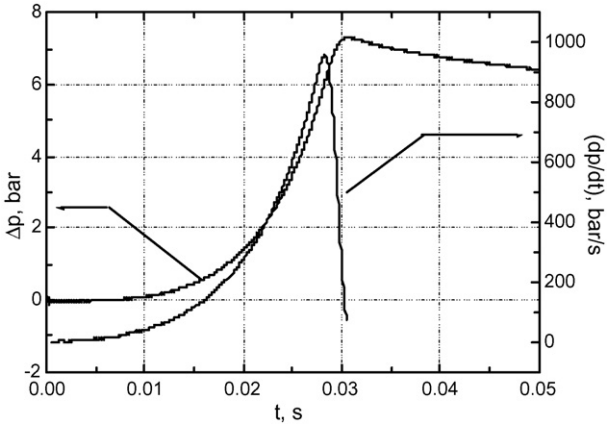

Fig. 1. Pressure evolution during the explosion of a lean C_3H_6–air mixture ($[C_3H_6] = 3.76$ vol.%, $\varphi = 0.837$) at $p_0 = 1$ bar, in vessel S, central ignition.

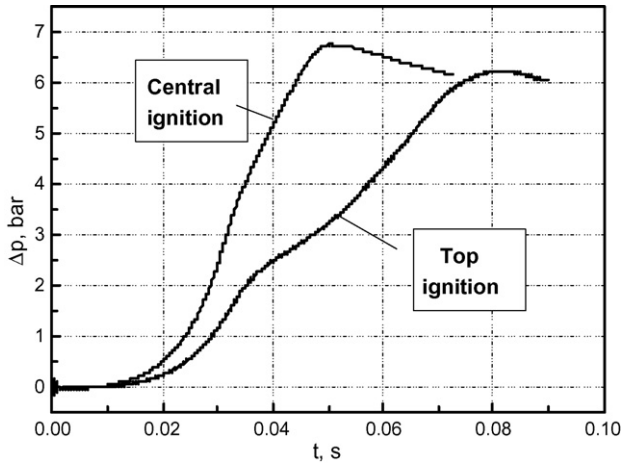

Fig. 2. Pressure evolution during the explosion of a lean C_3H_6–air mixture ($[C_3H_6] = 3.76$ vol.%, $\varphi = 0.837$) at $p_0 = 1$ bar, in vessel C; central and top ignition.

two sets of data measured in identical conditions, at ambient initial pressure and temperature was 2.1% for a 4.22% C_3H_6–air mixture ($(dp/dt)_{max} = 1224.2 \pm 25.4$ bar/s; 11 experiments) and 3.1% for a C_3H_6–air mixture ($(dp/dt)_{max} = (848.7 \pm 25.9$; nine experiments).

A set of two $p(t)$ diagrams recorded in cylindrical vessel C, at central and top ignition, respectively, are given in Fig. 2. For top ignitions, a break point is observed at the moment where the flame has reached the sidewall and propagates downwards; the important heat transfer in this stage leads to a much lower rate of pressure rise, as compared to the previous stage, of hemispherical propagation. For central ignition, the presence of the break point is less obvious. In both cases, we selected only data with $0 \leq t \leq 1.1 \times \theta_{break}$ and we applied the same calculation procedure as for spherical vessel.

3. Computing program

Calculations of adiabatic explosion pressure and flame temperature were made with the program ECHIMAD [29], based on a general algorithm meant to compute the equilibrium composition of products for any fuel–oxidizer gaseous mixture. The algorithm is based on the thermodynamic criterion of chemical equilibrium used by Gibbs: the minimum of free enthalpy, at constant temperature and pressure or minimum of free energy, at constant temperature and volume. Fifteen compounds, among them one solid compound ($C_{graphite}$) were considered as products: $C_{graphite}$, CO_2, CO, H_2O, O_2, N_2, CH_4, C_2H_2, C_2H_4, C_3H_6, H_2, NO, H, OH and O). Their heat capacities (expressed as function of temperature of the form: $C_p = a + bT + cT^2 + dT^{-2}$), the standard enthalpies of formation at 298 K and the standard entropies at 298 K were taken from literature [30,31].

4. Results and discussion

For explosions in spherical vessel, the peak values of ionization probe signal and of pressure rise are simultaneously reached, short time before the peak pressure appears. Only in the close

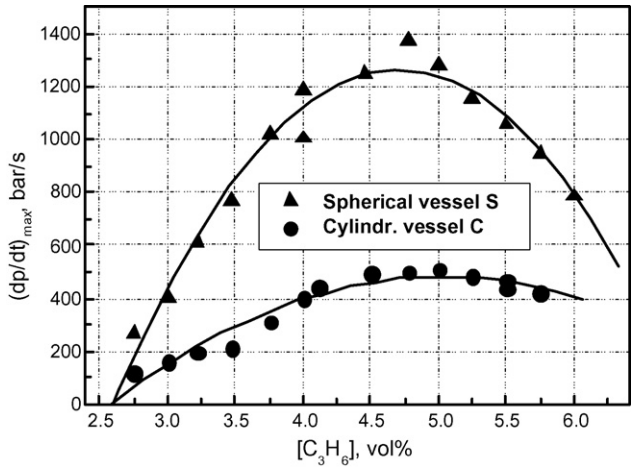

Fig. 3. Maximum rates of pressure rise for propylene–air explosions at $p_0 = 1$ bar and $T_0 = 298$ K, in spherical vessel S and in cylindrical vessel C.

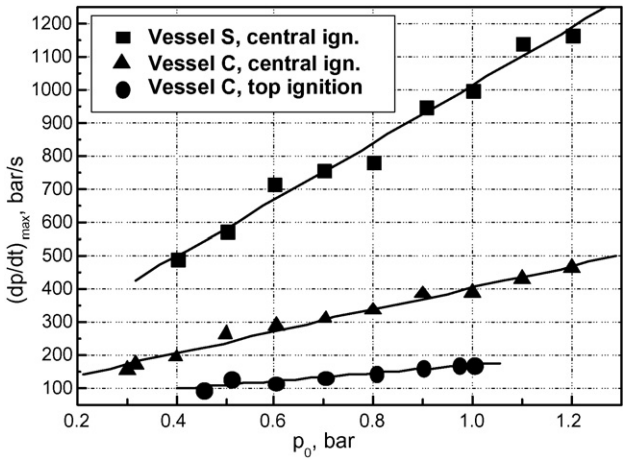

Fig. 4. Maximum rates of pressure rise, for explosions of a 4.46% C_3H_6–air mixture in vessels S and C, at various initial pressures and positions of ignition source.

vicinity of the wall heat loss starts, so that the real (measured) peak pressure is lower than the computed adiabatic value. The occurrence of a break point on the $p(t)$ records of explosions in cylindrical vessel C suggests that important heat losses start much earlier and have important values as compared to spherical vessel. Therefore, the maximum rates of pressure rise observed during explosions in cylindrical vessel C are systematically lower as compared to the rates observed during explosions in spherical vessel S. Data referring to propylene–air mixtures with variable propylene content at initial pressure $p_0 = 1$ bar, between the lower and upper flammability limit, are plotted in Fig. 3.

Both diagrams have a maximum situated in the range of rich mixtures ($[C_3H_6] = 4.5$–5.0 vol.%) characterized by the highest reactivity, as seen from similar diagrams of burning velocities versus fuel concentration [27,32]. Similar plots were obtained by plotting the maximum rates of pressure rise versus propylene concentration, at all values of initial pressure. In the vicinity of flammability limits, the maximum rates of pressure rise in the examined vessels have close values. Near the most reactive composition, the values of $(dp/dt)_{max}$ in vessel S have much higher values as compared to vessel C. Additional measurements performed in another cylindrical vessel with $h = Ø = 6$ cm and central ignition indicated $(dp/dt)_{max} = 1280$ bar/s for the stoichiometric mixture at $p_0 = 1$ bar, a value closer to those characteristic to the spherical vessel.

For each enclosure and each fuel/air ratio, the maximum rate of pressure rise follows a linear dependence on initial mixture pressure, as reported earlier for H_2–air, C_3H_8–air and C_5H_{12}–air mixtures [2] in the range of sub-atmospheric pressures and even at initial pressures higher than 1 bar (with the obvious limitation to deflagrative combustions). Representative results for a stoichiometric propylene–air mixture are given in Fig. 4, for spherical vessel S and cylindrical vessel C. Such diagrams are important for calculation of pressure rise rates at initial pressures different from ambient, but not outside the examined range of initial pressures.

Asymmetric ignition, at top of cylindrical vessel C, induces important heat losses during flame propagation. This process is characterized by the lowest rates of pressure rise, as compared to propagation of a flame ignited in the centre of the same vessel. The propagation in spherical vessel S is characterized by the greater rates of pressure rise, ranging from 550 bar/s at 0.5–1400 bar/s at 1 bar.

Values of maximum rates of pressure rise for other stoichiometric fuel–air mixtures at ambient initial pressure and temperature, taken from literature, are given in Table 1, for explosions in spherical [2] or quasi-spherical [7] vessels with central ignition. Their values range usually within 300–600 bar/s for alkane–air mixtures (e.g. CH_4–air, C_3H_8–air in a 5 L spherical vessel with central ignition [2]), but are much smaller when larger vessels are used. Quite high values, such as 3200 bar/s (H_2–air) and 8300 bar/s (C_2H_2–air) were measured in the 5 L spherical vessel with central ignition [2].

Our data concerning propylene–air mixtures are higher as compared to those referring to alkane–air mixtures, determined in spherical vessels of a close volume. Indeed, the larger is the evolved heat in the combustion process, the higher is the rate of pressure increase. This is confirmed by the plots in Fig. 5, where data refer to centrally ignited explosions in spherical vessel S of propylene–air mixtures with variable propylene content. Similar data acquired for explosions in cylindrical vessel C, at

Table 1
Maximum rates of pressure rise for explosions of stoichiometric fuel–air mixtures at ambient initial pressure and temperature, in spherical vessels with central ignition

Fuel	Volume	$\left(\frac{dp}{dt}\right)_{max}$ (bar/s)	Reference
CH_4	5 L	322	[2]
	0.5 m^3	100	[2]
	1.0 m^3	80	[2]
	26.5 m^3	36	[7]
C_3H_8	5 L	585	[2]
	0.5 m^3	200	[2]
H_2	5 L	3220	[2]
C_2H_2	5 L	8300	[2]

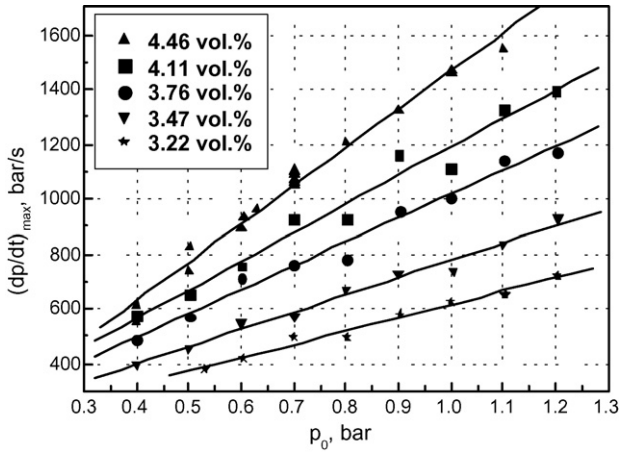

Fig. 5. Maximum rate of pressure rise in vessel S with central ignition, for several C_3H_6–air mixtures at various initial pressures.

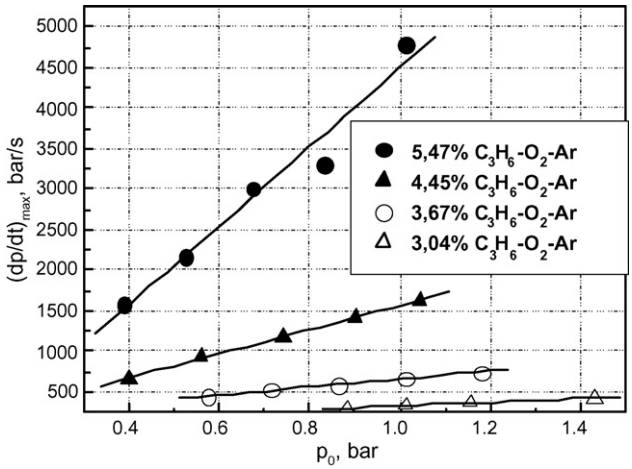

Fig. 7. Maximum rate of pressure rise in spherical vessel S with central ignition; C_3H_6–O_2–Ar stoichiometric mixtures.

central and top ignition, are given in Fig. 6. Larger heat losses for asymmetric ignition account for the systematic decrease of pressure rise rates as compared to central ignition.

Additional data referring to a stoichiometric propylene–oxygen mixture (constant mole ratio $C_3H_6/O_2 = 1/4.5$) diluted with various amounts of argon (within 70–83 vol.%) are given in Fig. 7. The increase of diluent concentration for the same total pressure entails the decrease of both slope and intercept of found linear correlation $(dp/dt)_{max}$ versus p_0. In Fig. 8, maximum rates of pressure rise for a stoichiometric propylene–oxygen mixture diluted with the same amount of inert (Ar and CO_2, 70 vol.%) are plotted.

Although the same amount of heat is released, the rates of pressure rise are very different, irrespective of initial pressure. Both chemical and physical effects contribute to this result. Both diluents change the thermo-physical properties of unburned mixture (thermal conductivity and heat capacity) and contribute to the decrease of flame temperature and heat transfer rate from flame to unburned mixture. Carbon dioxide is additionally involved in chemical equilibria within the flame front through its endothermic dissociation, having a larger effect on the rate of pressure rise.

The more pronounced inerting effect of carbon dioxide is also illustrated in Figs. 9 and 10, where the combustible mixture was diluted with exhaust gas, argon or carbon dioxide. Fig. 9 indicates that the maximum rate of pressure rise for propylene–air mixtures with variable equivalence ratio decreases with the increasing content of added exhaust gas. In Fig. 10, a comparison is given between stoichiometric propylene–air mixtures containing Ar, CO_2 or exhaust gas as diluents. The exhaust gas of a stoichiometric propylene–air mixture contains 13.1 vol.% CO_2, 13.1 vol.% H_2O and 73.8 vol.% N_2 (composition calculated for a cooled exhaust gas), therefore this gas acts through the inert component (N_2), water vapours and carbon dioxide. As seen, the rates of pressure rise for mixtures diluted by exhaust gas lie between those of Ar- and CO_2-diluted mixtures.

From the rates of pressure rise in enclosures with central ignition, the deflagration index K_G was calculated. Two sets of data obtained from measurements in spherical vessel S and in the smaller cylindrical vessel V ($h = \Phi$) were plotted in Fig. 11, as deflagration index versus initial pressure. The deviations

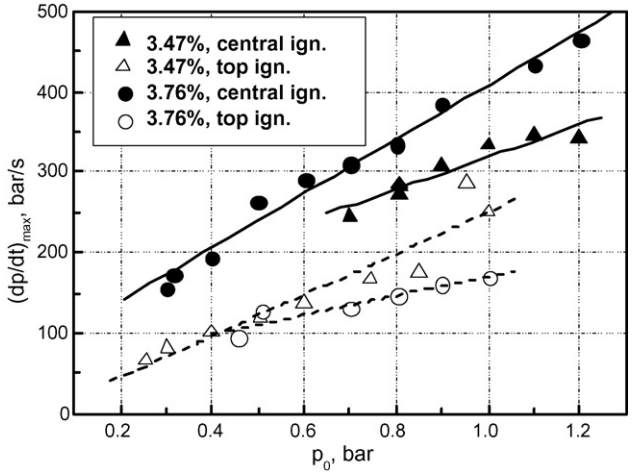

Fig. 6. Maximum rate of pressure rise in cylindrical vessel C with central and top ignition, for two C_3H_6–air mixtures at various initial pressures.

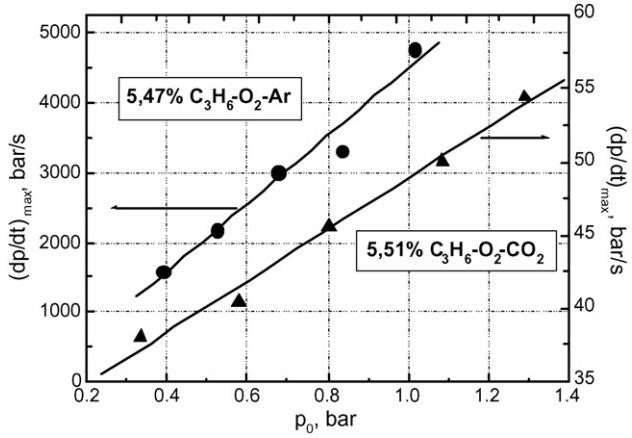

Fig. 8. Maximum rate of pressure rise in spherical vessel S with central ignition; stoichiometric mixtures C_3H_6–O_2 diluted with 70% inert (Ar or CO_2).

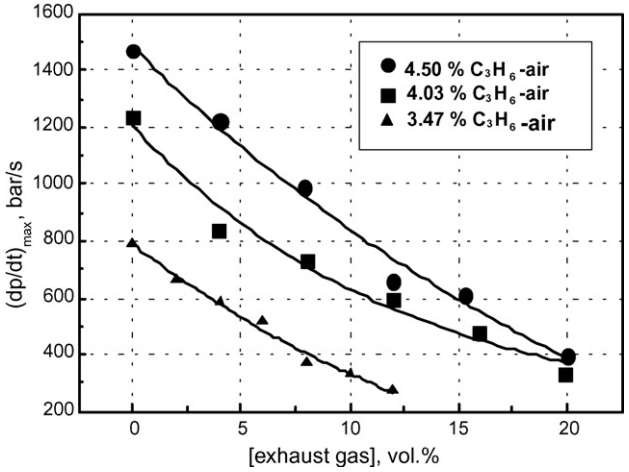

Fig. 9. Propylene–air mixtures diluted by their own exhaust gases; data measured in spherical vessel S, $p_0 = 1$ bar.

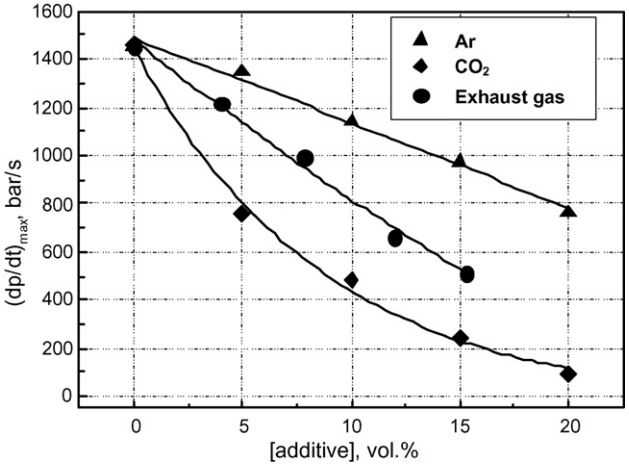

Fig. 10. Stoichiometric propylene–air mixtures diluted by additives; data measured in spherical vessel S at $p_0 = 1$ bar.

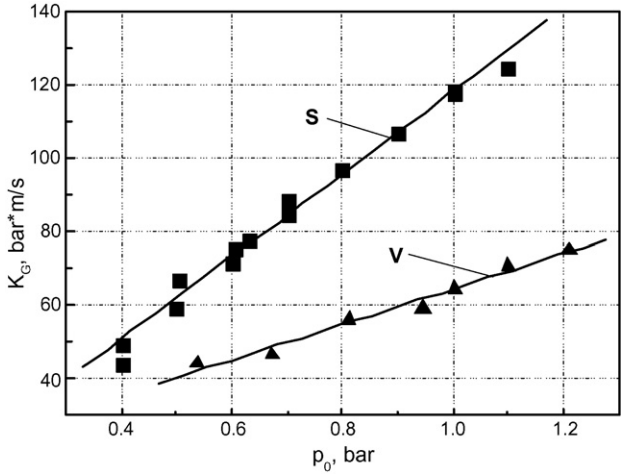

Fig. 11. Deflagration index of a stoichiometric C_3H_6–air mixture; spherical vessel S and cylindrical vessel V.

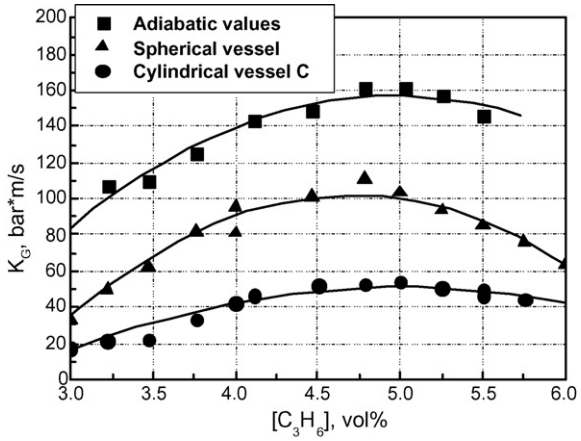

Fig. 12. Deflagration index of propylene–air mixtures: adiabatic values and data from experiments in spherical vessel S and cylindrical vessel C, central ignition.

between the deflagration indexes in these vessels are determined by both the difference between the volumes of these enclosures ($V_s = 0.52$ L; $V_v = 0.17$ L) and the difference between the ratio (lost heat/evolved heat) in the two vessels. For both sets of data, a linear correlation was found between the deflagration index and the initial pressure, in agreement with earlier results [2]. Similar plots were obtained for all examined compositions.

In Fig. 12, the deflagration index calculated for centrally ignited deflagrations in vessels S and V is plotted versus propylene concentration. Fig. 12 contains also the values of "adiabatic" deflagration index, K_{max}. K_{max} was calculated according to an equation derived by Dahoe et al. [32] and improved by van den Bulck [19] by means of data for several representative fuel–air mixtures, for a range of equivalence ratios, initial temperatures and initial pressures:

$$K_{max} = \frac{(36\pi)^{1/3}}{1.041}(p_{max} - p_0)\left(\frac{p_{max}}{p_0}\right)^{1/\gamma_u} S_f \quad (2)$$

Here, p_{max} is the adiabatic peak pressure, reached in explosions at initial pressure p_0; γ_u the adiabatic coefficient of unburned gas and S_f is the burning velocity of fuel–air mixture, at peak pressure. We calculated the burning velocity at peak explosion pressure, S_f, according to a power law equation:

$$S_f = S_{u,0}\left(\frac{T}{T_0}\right)^{\mu}\left(\frac{p}{p_0}\right)^{\nu} = S_{u,0}\left(\frac{p}{p_0}\right)^{\mu(1-1/\gamma_u)+\nu} \quad (3)$$

where $S_{u,0}$ is the laminar burning velocity at ambient initial conditions, μ the thermic coefficient and ν is the baric coefficient of burning velocity. Their values were taken from two recent publications [27,33]. The adiabatic explosion pressures were calculated with the program ECHIMAD, for propylene–air mixtures with variable propylene/air ratio, at constant initial pressure $p_0 = 1$ bar. The last term of Eq. (3) expressed the overall variation of laminar burning velocity during explosion only as a function of pressure, since the temperature and pressure of unburned gas are related by means of the adiabatic compression equation:

$$T = T_0\left(\frac{p}{p_0}\right)^{1-1/\gamma_u} \quad (4)$$

For all mixtures, the adiabatic values (K_{max}) lie above the "real" K_G values, calculated from experimental data. The differences between the index K_G of deflagration in the examined vessels *S* and *V* are not significant in the vicinity of flammability limits, but are quite great for the most reactive mixture. Due to such differences, a comparison between various fuel–air mixtures should be done using the adiabatic K_{max} values, especially when a "worst case" scenario has to be delivered.

Data from Figs. 5–10 can also be converted into plots of deflagration index against initial pressure. As long as these plots use only data from spherical vessel *S*, such new plots would not bring additional information.

5. Conclusions

In spherical and cylindrical vessels with central ignition, both $(dp/dt)_{max}$ and K_G are specifically influenced by the propylene content of flammable mixture, by the total initial pressure (at constant composition) and by addition of various components (at constant initial pressure). The highest values of maximum rate of pressure rise $(dp/dt)_{max}$ and of deflagration index K_G for deflagrations of propylene–air mixtures in several enclosures are observed in the spherical vessel with central ignition. The position of the ignition source – central or at top of the vessel – strongly influences the rate of pressure rise and the deflagration index. The higher heat losses associated to the asymmetric ignition (earlier contact of flame with top and sidewalls, as compared to central ignition) and the reduced flame front area determine lower rates of pressure rise.

At constant initial pressure and compositions near the flammability limits, the deflagration index of propylene–air mixtures for vessels S and C with central ignition have close values. When propylene content is close to the stoichiometric composition (equivalence ratio $\varphi = 1.1–1.2$), the deflagration indexes determined in vessel S are higher than the deflagration indexes determined in vessel C and both are exceeded by the adiabatic values K_{max}.

The reported measurements, made with a spherical vessel different from the EU standard (recommending a 20 L sphere), provide useful results concerning explosion evolution in propylene–air and propylene–oxygen inert systems. The data from the other vessels C and V might be also useful for scaling explosions in chemical reactors, which are in most cases cylindrical vessels.

Acknowledgement

This work was partly financed by Grant no. 42/2003-2004 awarded by the Romanian Academy to the Institute of Physical Chemistry Bucharest.

References

[1] EN 13673-2, Determination of maximum explosion pressure and the maximum rate of pressure rise of gases and vapours – Part 2: Determination of the maximum rate of explosion pressure rise, European Standard, Beuth Verlag, Berlin Wien Zurich, 2005.

[2] W. Bartknecht, G. Zwahlen, G. Explosionsschutz, Grundlagen und Anwendung, Springer–Verlag, Berlin, 1993.

[3] NFPA 68, Guide for Venting Deflagrations, 1998 ed., National Fire Protection Association, 1998.

[4] C. Mashuga, D. Crowl, Application of the flammability diagram for evaluation of fire and explosion hazards of flammable vapors, Proc. Safety Prog. 17 (1998) 176–183.

[5] D. Razus, U. Krause, Empirical and semi-empirical calculation methods for venting of gas explosions, Fire Safety J. 36 (2001) 1–23.

[6] J. Nagy, E. Seiler, J. Conn, H. Verakis, Explosion Development in a Spherical Vessel, U.S. Bureau of Mines Report of Investigation 7507, 1971.

[7] M. Sapko, A. Furno, J. Kuchta, Flame and Pressure Development of Large-Scale CH_4–Air–N_2 Explosions, U.S. Bureau of Mines Report of Investigation 8176, 1976.

[8] H. Phylaktou, G. Andrews, P. Herath, Fast flame speeds and rates of pressure rise in the initial period of gas explosions in large *L/D* cylindrical enclosures, J. Loss Prevent. Process Ind. 3 (1990) 355–364.

[9] H. Phylaktou, G. Andrews, Gas explosions in long closed vessels, Combust. Sci. Technol. 77 (1991) 27–39.

[10] K. Cashdollar, I. Zlochower, G. Green, R. Thomas, M. Hertzberg, Flammability of methane, propane, and hydrogen gases, J. Loss Prevent. Process Ind. 13 (2000) 327–340.

[11] Y. Tanaka, Numerical simulations of combustion of quiescent and turbulent mixtures in confined vessels, Combust. Flame 75 (1989) 23–138.

[12] C. Catlin, A. Manos, J. Tite, Mathematical modeling of confined explosions in empty cube and duct shaped enclosures, Trans. Inst. Chem. Eng. 71 (1993) 89–100 (Part B).

[13] U. Krause, Ein beitrag zur mathematischen modellierung des ablaufs von explosionen, BAM Forschungsbericht 194 (1993).

[14] D. Pritchard, D. Freeman, P. Guilbert, Prediction of explosion pressures in confined spaces, J. Loss Prevent. Process Ind. 9 (1996) 205–215.

[15] M. Fairweather, G. Hargrave, S. Ibrahim, D. Walker, Studies of premixed flame propagation in explosion tubes, Combust. Flame 116 (1999) 504–518.

[16] A. Dahoe, L. de Goey, On the determination of the laminar burning velocity from closed vessel gas explosions, J. Loss Prevent. Process Ind. 16 (2003) 457–478.

[17] D. Bradley, A. Mitcheson, Mathematical solutions for explosions in spherical vessels, Combust. Flame 26 (1976) 201–217.

[18] T. Takeno, T. Iijima, Theoretical study of non-steady flame propagation in closed vessels, in: Proceedings of the 7th International Colloquium on Gas Dynamics of Explosions and Reactive System, Göttingen, Germany, 1979, pp. 20–24.

[19] E. Van den Bulck, Closed algebraic expressions for the adiabatic limit value of the explosion constant in closed vessel combustion, J. Loss Prevent. Process Ind. 18 (2005) 35–42.

[20] B. Lewis, G. von Elbe, Combustion Flames and Explosion of Gases, 3rd ed., Academic Press, New York, 1987.

[21] H. Maisey, Gaseous and Dust Explosion Venting, Chem. Proc. Eng. (1965) 527–563.

[22] A. Furno, E. Cook, J. Kuchta, D. Burgess, Proceedings of the 13th Symposium (International) on Combustion, The Combustion Institute, 1971, pp. 593–599.

[23] G. Andrews, P. Herath, H. Phylaktou, The influence of flow blockage on the rate of pressure rise in large *L/D* cylindrical closed vessel explosions, J. Loss Prevent. Process Ind. 3 (1990) 291–302.

[24] Y. Lisochkin, V. Poznyak, V. Rykuniov, Explosion parameters of gaseous fluorinated monomers and their mixtures burning in a closed vessel, Chem. Phys. Rep. 17 (1999) 2157–2162.

[25] Yu.N. Shebeko, V.V. Azatyan, I.A. Bolodian, V. Yu Navzenya, S.N. Kopylov, D. Yu.Shebeko, E.D. Zamishevski, The influence of fluorinated hydrocarbons on the combustion of gaseous mixtures in a closed vessel, Combust. Flame 121 (2000) 542–547.

[26] M. Gieras, R. Klemens, G. Rarata, P. Wolanski, Determination of explosion parameters of methane–air mixtures in the chamber of 40 dm^3 at normal and elevated temperature, J. Loss Prevent. Process Ind. 19 (2006) 263–270.

[27] D. Razus, D. Oancea, C. Movileanu, Pressure evolution during the early stage of closed-vessel explosions, J. Loss Prevent. Process Ind. 19 (2006) 334–342.

[28] D. Razus, C. Movileanu, V. Brinzea, D. Oancea, Explosion pressures of hydrocarbon–air mixtures in closed vessels, J. Hazard. Mater. 135 (2006) 58–65.

[29] D. Geana, D. Popescu, M. Mihai, L. Adomnica, Computation of equilibrium temperature and composition during adiabatic combustion, Rev. Chim. 36 (1985) 708–714.

[30] D. Stull, E. Westrum Jr., G. Sinke, The Chemical Thermodynamics of Organic Compounds, Wiley & Sons, New York, 1969.

[31] O. Knacke, O. Kubaschewski, K. Hesselman, Thermochemical Properties of Inorganic Substances, 2nd ed., Springer–Verlag, Berlin, 1991.

[32] A. Dahoe, J. Zevenbergen, S. Lemkowitz, B. Scarlett, Dust explosions in spherical vessels: the role of flame thickness in the validity of the cube-root law, J. Loss Prevent. Process Ind. 9 (1996) 33–44.

[33] D. Razus, D. Oancea, N.I. Ionescu, Burning velocity determination by spherical bomb technique. Part II. Application to gaseous propylene–air mixtures of various compositions, pressures and temperatures, Rev. Roum. Chim. 45 (2000) 319–330.